JSACE 2/40

Influence of Response Acceleration-Dependent Damping on the Nonlinear Seismic Behavior of Reinforced Concrete Columns

Received 2026/01/24

Accepted after revision 2026/05/20

Influence of Response Acceleration-Dependent Damping on the Nonlinear Seismic Behavior of Reinforced Concrete Columns

Maryam Alibraheem[1]*, Soleman Alamoudi[2]

[1] Department of Structural Civil Engineering, Homs University, Homs, Syria.

[2] Department of Structural Civil Engineering, Homs University, Homs, Syria.

*Corresponding author: **maryam2022ib@gmail.com**

https://doi.org/10.5755/j01.sace.44132

Abstract

Accurately representing damping remains a major challenge in nonlinear seismic analysis of reinforced concrete (RC) elements, particularly under severe ground motions where stiffness degradation invalidates the assumptions of conventional models. Classical Rayleigh damping, despite its widespread use, often produces spurious energy dissipation and inaccurate response predictions in inelastic systems.

To address this limitation, this study proposes acceleration-dependent damping formulations in which damping evolves at each time step according to the instantaneous structural response. The proposed approach is implemented within a nonlinear time history analysis framework using direct integration. An RC column model based on distributed plasticity is developed by discretizing the member into multiple sub-elements to accurately capture inelastic behavior. Four damping models are investigated: Model A employs classical Rayleigh damping with constant coefficients based on initial stiffness and a fixed 5% damping ratio; Models B and C apply acceleration-updated Rayleigh damping, where Model B retains initial stiffness and Model C incorporates tangent stiffness; Model D introduces a fully response-driven diagonal damping matrix that varies directly with response acceleration over time.

The analytical results are validated against ETABS simulations and experimental data from shake table tests of an RC column subjected to scaled records of the 1994 Kushiro earthquake. Compared with conventional damping, the proposed acceleration-dependent models significantly reduce prediction errors and eliminate non-physical damping effects. Models B and C achieved deviations between −8.9% and +3.2%, while Model D further improved accuracy, limiting peak acceleration deviations to −8.11% and +2.3%.

The results demonstrate that coupling damping evolution with instantaneous response provides a physically consistent and numerically robust alternative to classical approaches. The novelty

ktu 1922

Journal of Sustainable Architecture and Civil Engineering
Vol. 2 / No. 40 / 2026
pp. 88-98
DOI 10.5755/J01.SACE.44132

of this study lies in the formulation and validation of time-dependent, acceleration-driven damping models that dynamically adapt during analysis, enabling more accurate prediction of nonlinear seismic response in degrading RC systems without reliance on empirically fixed damping assumptions.

Keywords: nonlinear seismic analysis; RC columns; time history analysis; variable damping.

Introduction

Nonlinear seismic analysis is essential for capturing the true behavior of reinforced concrete structures under earthquake-induced demands, which are often highly dynamic and complex. Unlike linear models, nonlinear approaches allow for a more realistic representation of material and structural responses, especially under extreme loading conditions. Two key aspects govern the reliability of nonlinear seismic analysis. The first is the adoption of robust seismic design methodologies to ensure structural safety under earthquake loading (Abdulahad & Danhash, 2025; Abdulahad & Grancharov, 2024; Ghassoun et al., 2023; Mahmud & Abdulahad, 2022; Mahmud et al., 2019). The second is the accurate representation of material behavior within finite element models to obtain reliable analytical predictions (Ghassoun et al., 2023). Incorporating response-dependent damping evolution into nonlinear analysis can further improve predictive accuracy by capturing the changing energy dissipation characteristics during seismic loading. This refinement supports a deeper understanding of column performance and informs more effective design strategies aimed at reducing collapse risk and improving overall structural resilience.

Experimental investigations and field observations, such as those by Chopra and McKenna (2015), confirmed that damping characteristics were closely tied to a structure's seismic response. Research by Alsehnawi et al. (2014) and Ghassoun and Alsehnawi (2023) revealed that damping ratios in the elastic phase ranged between 2–3%, increasing progressively with amplitude and nonlinearity. Similarly, Kowalsky (1994) observed that damping in concrete structures started below 3% and could rise to 7–8% with significant cracking and nonlinear behavior. Priestley et al. (2007) cautioned that assuming a fixed 5% damping ratio in seismic analysis could overestimate damping and underestimate dynamic response.

Alsehnawi et al. (2014) further investigated the dependence of dynamic properties on vibration amplitude through free vibration tests on reinforced concrete pier models. These tests were conducted across a wide amplitude range, initially on intact specimens, then after progressive damage on a shake table, and finally after repairs using epoxy and carbon fiber strips.

Their findings showed that damping ratios increased significantly with higher acceleration amplitudes, while natural frequencies decreased slightly. Ghassoun (2020a) later analyzed these experimental results to derive relationships linking dynamic properties; namely natural frequency and damping ratio; to maximum response acceleration across different specimen conditions, including intact, cracked, and repaired states.

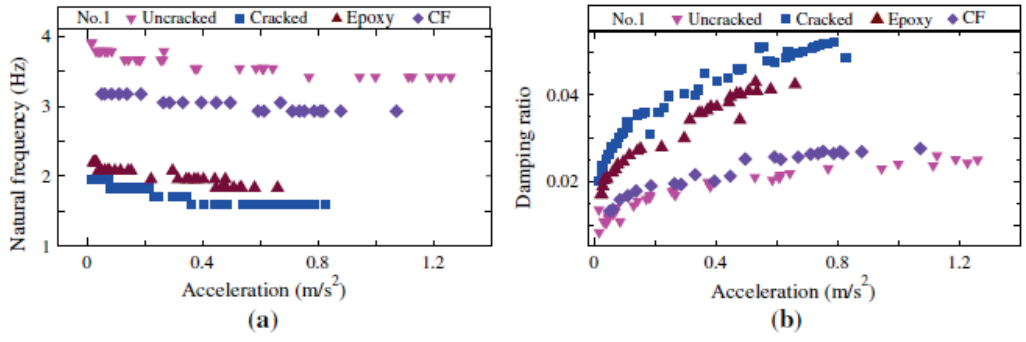


Fig. 1
Variation of natural frequency **a** and damping ratio **b** with maximum response acceleration (Alsehnawi et al., 2014)

The proposed relationship in the case of intact (non-cracked) samples was as follows (Ghassoun, 2020a):

$$\begin{aligned} 0.01 \le |\ddot{u}| \le 0.05 &\Rightarrow \xi = 0.148|\ddot{u}| + 0.008 \\ 0.05 < |\ddot{u}| \le 1.27 &\Rightarrow \xi = -0.01|\ddot{u}|^2 + 0.023|\ddot{u}| + 0.017 \\ |\ddot{u}| > 1.27 &\Rightarrow \xi = 0.0338 \end{aligned} \quad (1)$$

While the proposed relationship in the case of cracked samples is as follows (Ghassoun, 2020a):

$$\begin{aligned} 0.003 \le |\ddot{u}| \le 0.06 &\Rightarrow \xi = 0.174|\ddot{u}| + 0.009 \\ 0.06 < |\ddot{u}| \le 0.8 &\Rightarrow \xi = -0.035|\ddot{u}|^2 + 0.05|\ddot{u}| + 0.019 \\ |\ddot{u}| > 1.27 &\Rightarrow \xi = 0.0365 \end{aligned} \quad (2)$$

Where: - the maximum response acceleration ; ξ - the damping ratio

This study proposes a nonlinear seismic analysis framework that incorporates distributed plasticity and acceleration-dependent damping evolution within direct integration time-history analysis.. The proposed methodology was implemented using special analysis software designed for this purpose, so that both the stiffness matrix and the damping matrix are updated instantaneously depending on the response values. In order to verify the effectiveness of the proposed methodology, it was applied to the RC pier model contained in the reference study by Alsehnawi et al. (2014), where the pier was loaded onto a vibration platform at different intensities of the Kushiro 1994 earthquake. The pier was analyzed at the intensities that caused it to enter the nonlinear field, which are 50% - 100% - 150% - 160%. Comparing the experimental acceleration values with the analytical values in the cases of constant damping and variable damping.

Several researchers have highlighted the limitations of classical viscous damping models in nonlinear seismic analysis. Hall (2006) demonstrated that Rayleigh damping may generate excessive and non-physical damping forces when structural stiffness degrades during inelastic response. Similarly, Charney (2008) showed that inappropriate damping modeling can significantly distort nonlinear dynamic response predictions and lead to unconservative analytical results. Chopra and McKenna (2015) further emphasized that conventional stiffness-proportional damping formulations may become unreliable in nonlinear response-history analysis due to the continuous evolution of structural properties under severe seismic loading.

Experimental and analytical investigations have also attempted to improve damping representation in degrading reinforced concrete systems. Petrini et al. (2008) verified that damping assumptions strongly influence the accuracy of nonlinear time-history analysis, particularly after cracking and stiffness deterioration. Zareian and Medina (2010) proposed practical approaches for reducing unintended damping effects in inelastic structural systems; however, most existing approaches still rely on predefined damping assumptions that remain insensitive to instantaneous response evolution.

Although several studies investigated damping variation in reinforced concrete systems, most nonlinear seismic analyses still rely on fixed Rayleigh damping assumptions, which may introduce non-physical damping forces under stiffness degradation. Limited studies have explored acceleration-dependent damping formulations integrated within nonlinear direct time-history analysis of degrading RC members. Therefore, this study proposes and validates a time-dependent damping approach linked directly to instantaneous response acceleration.

Methods

Experimental program:

The adopted experimental model is a reinforced concrete bridge pier consisting of a column, cap and footing tested by Alsehnawi et al. (2014). Longitudinal reinforcement extends to the bottom of the base to provide sufficient resistance to moments at the base of the column, and the connection between the column and the cap is effectively continuous. An additional concrete block was used to simulate the top of the bridge at the top of the column. The cross-section of the column was rectangular with dimensions of (100×150) mm and a net height of 1500 mm. The cap section was rectangular with dimensions of (300×350) mm and a height of 100 mm. The footing section and upper block were (600×600) mm with a height of 200 mm (Fig. 2). The column reinforcement consisted of four bars with a diameter of 10 mm, equivalent to a reinforcement ratio of 2.08%, and hoops with a diameter of 6 mm, distributed with a spacing of 100 mm at the top and bottom of the column up to 300 mm, while the spacing was 200 mm in the middle of the column. Four additional bars were added at the contact points between the column and the base, as well as at the column heads, 100 mm long from the contact surface, to avoid cracks in that area. The covering layer in all sections was adopted as 15 mm. The yield stress of reinforcing bars is 401 MPa and the modulus of elasticity is 210 kN/mm^2. While the resistance of the concrete to pressure and tension for the first sample, during the experiment period of 127 days, was 32.5 MPa and 2.68 MPa, respectively, and the elastic modulus was 31.9 kN/mm^2. While for the second sample, during the experiment period of 155 days, the resistances to pressure and tension were 31.8 MPa and 2.3 MPa and the modulus of elasticity was 29.1 kN/mm^2, and Fig. 2 shows the structural details of the tested model.

The researchers studied the effect of different damage scenarios on the dynamic properties of each sample by applying excitation with a shaking table that creates gradual damage and checking the normal frequency values and damping ratio of each model after damage occurs. To represent medium and strong seismic motions, each sample was excited by a miniature ground motion simulating the 1994 Kushiro earthquake with a maximum acceleration value of PGA=0.7g. This excitation was carried out according to different intensities, from which we will analytically study the intensities of 50% - 100% - 150% - 160%, as these intensities caused the substrate to enter the nonlinear field.

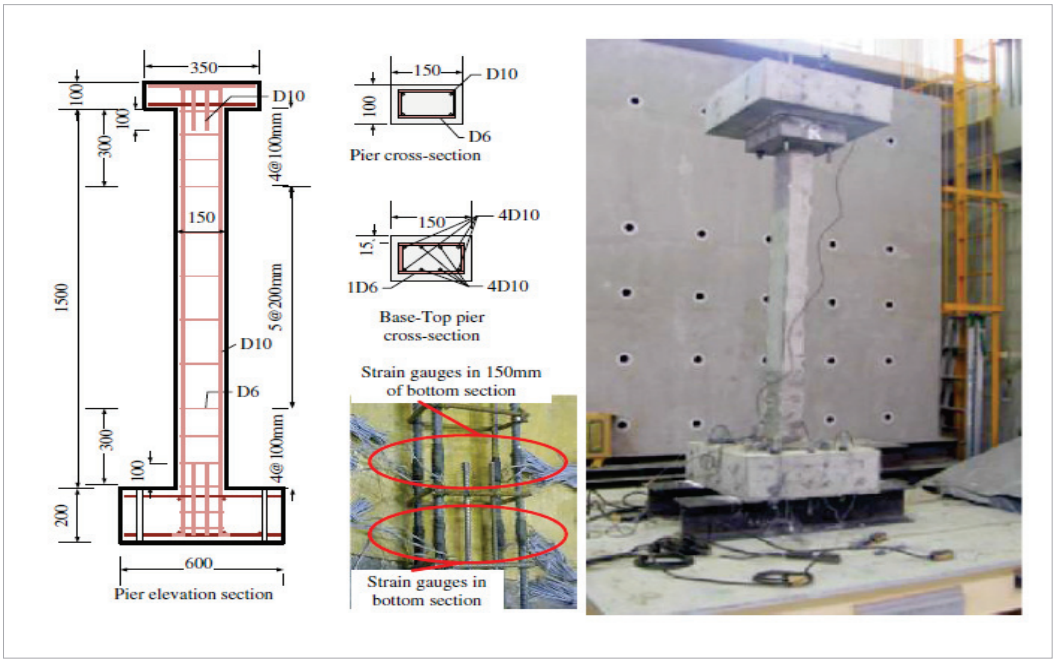


Fig. 2

Structural details of the model tested in the study by Alsehnawi et al. (2014)

Proposed methodology for introducing the effect of nonlinearity on seismic analysis:

The following methodology has been proposed to perform nonlinear analysis, and this methodology remains valid for use depending on the number of elements of the frame sentence. The steps of nonlinear analysis can be summarized as follows:

1. Definition of the studied element in terms of geometric dimensions, sections, and materials used.
2. Dividing the studied element into a group of partial elements (in this research, the division into 10 partial elements was relied upon)
3. Calculate the stiffness matrix for each partial element, then collect the stiffness matrices for these elements to obtain the total matrix of the element.
4. Obtain both the initial stiffness [K_0] and mass [M] matrices so that they are proportional to the degrees of freedom to be studied (the model was studied as a plane model so the degrees of freedom u, w,θ_y were relied upon).
5. Obtaining the damping matrix [C] and we will explain later the proposed methods for forming it.
6. Calculating the values of displacements, velocities, and accelerations at each moment in time based on the successive approximation method, assuming constant acceleration, which is one of the special cases of the Newmark method.
7. After calculating the displacements, the internal stresses occurring in each sub-element are calculated and both the elastic deformations ε_e are calculated based on the material resistance relationships at the maximum compressed concrete fiber and the actual deformations ε_c through the performance curves p-ε_c obtained for the intermediate sections in each sub-element based on a special program for analyzing the section according to the stress state to which it is exposed.
8. After calculating the values of elastic and actual deformations, the reduction coefficient of the stiffness matrix of each partial element is calculated as follows:

$$k = \frac{\varepsilon_e}{0.9\,\varepsilon_c} \leq 1 \qquad (3)$$

The matrix of each partial element is multiplied by the appropriate reduction factor and then the stiffness matrices are reassembled to obtain the new matrix of the studied element.

10. Based on the new stiffness matrix [K_t], the displacements, forces and accelerations are calculated again, and based on the accelerations, the damping matrix is calculated according to each of the proposed methods.
11. At each moment in time, we continue the calculation cycles until the percentage difference between transitions and accelerations in the new cycle does not exceed 5% of the previous cycle, then we move to the next time step.

Proposed methods for forming the damping matrix [C]:

In order to introduce the effect of variable damping on nonlinear analysis, the following methods have been proposed to form the damping matrix:

Method A: Forming the damping matrix based on the Rayleigh damping model [C]=α_0.[M]+α_1 [K_0] so that the coefficients α_0 and α_1 are calculated at a constant damping ratio ξ=5% and [K_0] the initial stiffness.

Method B: Forming the damping matrix based on the Rayleigh damping model [C]=α_0.[M]+α_1 [K_0] such that the coefficients α_0 and α_1 are calculated at a variable damping ratio related to the response acceleration ξ=f(ü) where they are calculated from **Eq. 1** if the element is not cracked and from **Eq. 2** if the element is cracked, and [K_0] the initial stiffness.

Method C: Forming the damping matrix based on the Rayleigh damping model $[C]=\alpha_0.[M]+\alpha_1[K_t]$ such that the coefficients α_0 and α_1 are calculated at a variable damping ratio related to the response acceleration $\xi=f(\ddot{u})$ where they are calculated from **Eq. 1** if the element is not cracked and from **Eq. 2** if the element is cracked, and $[K_t]$ represents the stiffness matrix of the element at each moment in time according to the stress state of the element.

Method D: Forming a damping matrix independent of stiffness. A shape for this matrix has been proposed as follows:

$$[C] = \begin{bmatrix} 2\varepsilon M_1 & 0 & 0 \\ 0 & 2\varepsilon M_2 & 0 \\ 0 & 0 & 2\varepsilon M_3 \end{bmatrix} \quad (4)$$

Where: ε - the damping coefficient

In order to determine the value of the damping coefficient, the experimental results of intact samples (**Fig. 3**) and cracked samples (**Fig. 4**) that were tested in the reference study by Alsehnawi et al. (2014) were processed.

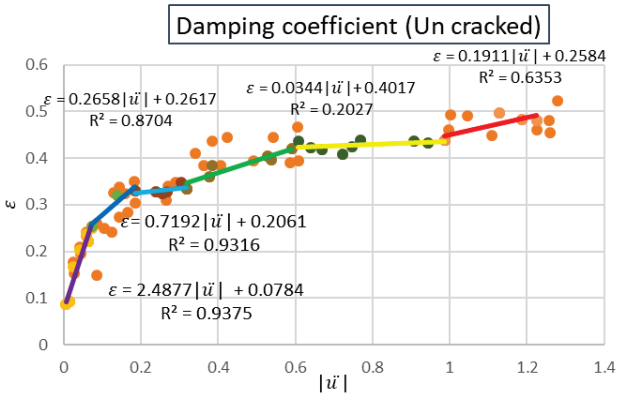


Fig. 3

Relationship between damping coefficient and response acceleration for intact specimens (un cracked)

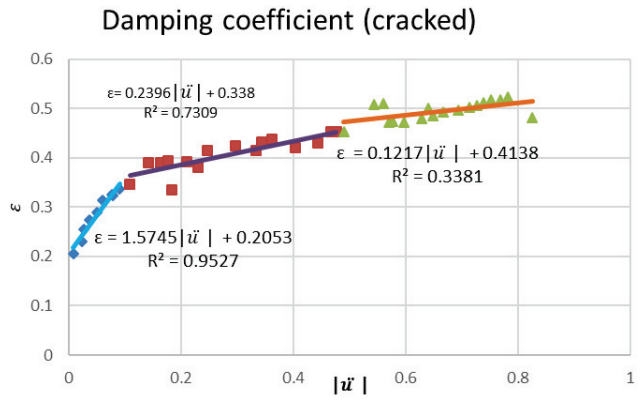


Fig. 4

Relationship between damping coefficient and response acceleration for cracked specimens

Based on the previous treatment, **Eq. 5** gives the values of the damping coefficient based on the acceleration of the response in the case of intact samples (Alibraheem & Amoudi, 2024), while **Eq. 6** gives the values of the damping coefficient based on the acceleration of the response in the case of cracked samples.

$$\begin{aligned}
|\ddot{u}| \le 0.0725 &\Rightarrow \varepsilon = 2.4877|\ddot{u}| + 0.0784 \\
0.0725 < |\ddot{u}| \le 0.18 &\Rightarrow \varepsilon = 0.7192|\ddot{u}| + 0.2061 \\
0.18 < |\ddot{u}| \le 0.3186 &\Rightarrow \varepsilon = 0.0885|\ddot{u}| + 0.31 \\
0.3186 < |\ddot{u}| \le 0.591 &\Rightarrow \varepsilon = 0.2658|\ddot{u}| + 0.2617 \\
0.591 < |\ddot{u}| \le 0.896 &\Rightarrow \varepsilon = 0.0344|\ddot{u}| + 0.4017 \\
0.896 < |\ddot{u}| \le 1.225 &\Rightarrow \varepsilon = 0.1911|\ddot{u}| + 0.2584 \\
|\ddot{u}| > 1.225 &\Rightarrow \varepsilon = 0.48
\end{aligned} \tag{5}$$

$$\begin{aligned}
|\ddot{u}| \le 0.09 &\Rightarrow \varepsilon = 1.5745|\ddot{u}| + 0.2053 \\
0.09 < |\ddot{u}| \le 0.48 &\Rightarrow \varepsilon = 0.2396|\ddot{u}| + 0.338 \\
0.48 < |\ddot{u}| \le 0.82 &\Rightarrow \varepsilon = 0.1217|\ddot{u}| + 0.4138 \\
|\ddot{u}| > 0.82 &\Rightarrow \varepsilon = 0.52
\end{aligned} \tag{6}$$

Time-history integration procedure:

The time history analysis method is based on performing a direct numerical integration of the equation of motion with time, under the influence of a time history representing seismic motion. This type of analysis allows the effect of nonlinearity to be introduced into materials and elements, and is also the most effective way to analyze irregular structures in terms of mass or stiffness.

In seismic analysis using the time log method, the equation of motion is solved directly using Numerical Integration Methods in order to obtain the seismic response of the structure under the influence of seismic motion. The method of successive approximation using the constant acceleration hypothesis is one of the special cases of the New mark method of numerical integration, and it is the most widespread in engineering applications due to its high numerical stability.

The steps of linear analysis using the time history method can be summarized as follows:

[1] forming both the stiffness and mass matrices.

[2] Formation of the damping matrix.

[3] At the time instant t=0 we assume that $u(0) = u(0) = \ddot{u(0)} = 0$

[4] At the moment in time t:

_ We calculate the equivalent force vector:

$$\overrightarrow{P_э}(t) = -[M] \times \overrightarrow{\ddot{u}_g}(t) \tag{7}$$

Where: -the beam of ground accelerations at the time instant t ; [M] - the mass matrix.

_ We calculate the equivalent stiffness matrix:

$$R_э(t) = \frac{4}{\Delta t^2}[M] + \frac{2}{\Delta t}[C] + [K] \tag{8}$$

Where: Δt - the time interval ; [M] - is the mass matrix ; [C] - the damping matrix ; [K] - the stiffness matrix

_ We calculate displacements, velocities, and accelerations from the following equations:

$$\vec{u}(t) = R_э(t) \times \overrightarrow{P_э}(t) \tag{9}$$

$$\vec{\dot{u}}(t) = \frac{2}{\Delta t}\vec{u}(t) \tag{10}$$

$$\vec{\ddot{u}}(t) = \frac{4}{\Delta t^2}\vec{u}(t) \tag{11}$$

[5] At the moment in time t+Δt:

_ We calculate the equivalent force vector:

$$\overrightarrow{P_3}(t+\Delta t) = -[M]\times\overrightarrow{\ddot{u}_g}(t+\Delta t) + \left(\frac{4}{\Delta t^2}[M] + \frac{2}{\Delta t}[C]\right)\vec{u}(t) + \left(\frac{4}{\Delta t}[M] + [C]\right)\vec{\dot{u}}(t) + [M]\vec{\ddot{u}}(t) \quad (12)$$

We calculate the equivalent stiffness matrix:

$$R_3(t+\Delta t) = \frac{4}{\Delta t^2}[M] + \frac{2}{\Delta t}[C] + [K] \quad (13)$$

We calculate displacements , velocities, and accelerations from the following equations:

$$\vec{u}(t+\Delta t) = R_3(t+\Delta t)\times\overrightarrow{P_3}(t+\Delta t) \quad (14)$$

$$\vec{\dot{u}}(t+\Delta t) = \frac{2\vec{u}(t+\Delta t) - 2\vec{u}(t) - \vec{\dot{u}}(t)\times\Delta t}{\Delta t} \quad (15)$$

$$\vec{\ddot{u}}(t+\Delta t) = \frac{4}{\Delta t^2}\left[\vec{u}(t+\Delta t) - \vec{u}(t) - \vec{\dot{u}}(t)\times\Delta t\right] - \vec{\ddot{u}}(t) \quad (16)$$

We repeat this step until the end of the analysis time.

Results

Based on the proposed nonlinear analysis methodology and the developed damping formulations, the reinforced concrete column experimentally investigated by Alsehnawi et al. (2014) was analyzed under scaled intensities (50%, 100%, 150%, and 160%) of the 1994 Kushiro earthquake. These loading levels were selected to ensure that the structural response entered the nonlinear range.

In order to compare the previous methodology with the results of nonlinear analysis in the ETABS program, the model was analyzed at each of the studied nonlinear intensities using the direct integration method with the definition of damping according to the Rayleigh damping model assuming a constant damping ratio ξ=5%.

Table 1 shows the maximum acceleration values resulting from the analysis according to the proposed methods compared with the experimental values at each seismic intensity, while Table 2 shows the percentage difference between analytical values and experimental values.

Table 1

Comparison of the values of the analytical accelerations with the experimental ones for the studied model by unit (m/sec2)

Seismic Intensity from Kushiro earthquake	$\ddot{u}_g/g$	Maximum experimental acceleration (m/sec^2)	Maximum acceleration result by ETABS (m/sec^2)	Maximum acceleration result by The program designed (m/sec^2)			
				Method A	Method B	Method C	Method D
50%	0.363	6.541	6.2	5.9	6.612	6.685	6.69
100%	0.727	11.545	12.4	11.283	11.918	11.92	10.88
150%	1.091	11.46	14.3	12.04	11.528	11.526	11.173
160%	1.163	13.2	14.7	11.55	12.028	12.07	12.13

Table 2

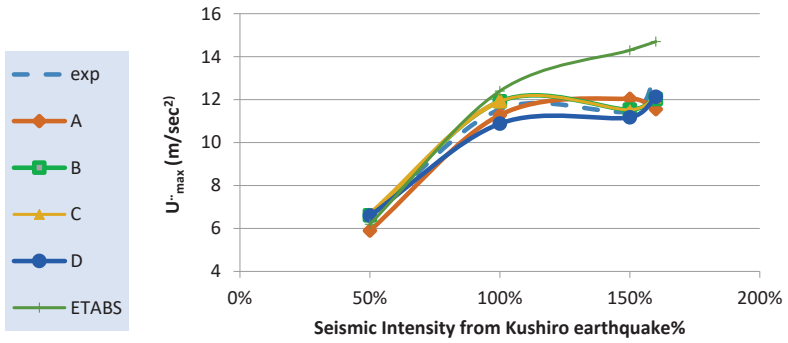
The difference between analytical and experimental maximum acceleration values (%)

Seismic Intensity from Kushiro earthquake	Maximum acceleration result by ETABS	Maximum acceleration result by The program designed			
		Method A	Method B	Method C	Method D
50%	-5.21%	-9.8%	+1.085%	+2.2%	+2.277%
100%	+7.406%	-2.27%	+3.2%	+3.2%	-5.76%
150%	+24.8%	+5.06%	+0.59%	+0.58%	-2.5%
160%	+11.36%	-12.5%	-8.88%	-8.56%	-8.11%

Fig. 5 shows the change in the values of the maximum accelerations resulting from the analysis with the change in seismic intensity compared to the experimental values.

Fig. 5

Analytical versus experimental maximum accelerations under different seismic intensities



Discussion

As shown in Fig. 5, the proposed nonlinear analysis methodology based on distributed plasticity along the entire element length provided closer agreement with the experimental results compared with the ETABS analysis, which relies on concentrated plastic hinges at the element ends while the remaining sections remain elastic. The difference between the two approaches became more pronounced under higher seismic intensities, where nonlinear effects and stiffness degradation were significantly amplified.

The proposed variable damping formulations based on Rayleigh damping (Methods B and C) also demonstrated improved accuracy compared with conventional constant damping assumptions. The prediction deviations ranged from –8.9% to +3.2%, indicating that incorporating acceleration-dependent damping evolution enhanced the reliability of the nonlinear response prediction. Moreover, the use of initial stiffness in Method B and tangent stiffness in Method C did not produce substantial differences in the analytical results.

Method D consistently produced the lowest prediction errors because the damping matrix evolved directly with the instantaneous acceleration response, thereby avoiding the excessive and non-physical damping forces commonly associated with stiffness-proportional Rayleigh damping under nonlinear degradation.

Conclusions

1. The results of the study showed that the proposed methodology for conducting nonlinear analysis, which relies on the distribution of plasticity over the entire length of the structural element, gave results closer to the experimental results than the method that relies on forming plastic joints at the ends of the elements while the remaining sections remain elastic.
2. Introducing the effect of variable damping associated with response acceleration into the formation of the damping matrix by calculating Rayleigh damping coefficients based on a variable damping ratio at each moment in time and thus modifying the damping matrix during the analysis gave results close to the experiment compared to calculating the coefficients based on a fixed damping ratio of 5%.
3. Forming the damping matrix independently of the stiffness matrix and based on the damping coefficient, which relates to the response acceleration at each time point, also gave results close to the experimental results, as the difference did not exceed 8.11%. Therefore, this method can be relied upon to form a variable damping matrix during analysis related to the response acceleration.
4. The findings demonstrate that response-dependent damping evolution can provide a practical and reliable framework for improving nonlinear seismic analysis of degrading reinforced concrete systems subjected to strong earthquake excitation.

The proposed methodology was validated using a single RC column configuration subjected to one earthquake record. Future studies may extend the approach to multi-degree-of-freedom systems, different structural typologies, and a wider range of seismic excitations to further evaluate the general applicability of the proposed damping formulations.

AI USE declaration

The authors used artificial intelligence (AI)-based tools solely for language editing and improving the clarity of the manuscript. The authors reviewed and approved all AI-assisted content and take full responsibility for the final manuscript.

References

Abdulahad, E. G., & Danhash, G. (2025). Recommendations for seismic assessment of heritage buildings and methods of strengthening. In Protection of Historical Constructions (Lecture Notes in Civil Engineering). Springer. https://doi.org/10.1007/978-3-031-87312-6_14

Abdulahad, E. G., & Grancharov, A. (2024). Seismic design of an existing six story administrative building. IOP Conference Series: Materials Science and Engineering, 1323(1), 012016. https://doi.org/10.1088/1757-899X/1323/1/012016

Alibraheem, M., & Amoudi, S. (2024). Effect of damping change with response acceleration in seismic analysis of a reinforced concrete frame. Homs University Journal, 46(5)

Alsehnawi, R., Nakajima, A., Takeshima, R., & Al Sadeq, H. (2014). Experimental investigation of amplitude dependency of dynamic characteristics in elastic and inelastic stages of reinforced concrete pier model. Journal of Civil Structural Health Monitoring, 4(3), 289-301. https://doi.org/10.1007/s13349-014-0092-5

Charney, F. A. (2008). Unintended consequences of modeling damping in structures. Journal of Structural Engineering, 134(4), 581-592. https://doi.org/10.1061/(ASCE)0733-9445(2008)134:4(581)

Chopra, A. K., & McKenna, F. (2015). Modeling viscous damping in nonlinear response history analysis of buildings for earthquake excitation. Earthquake Engineering & Structural Dynamics, 44(11), 193-211. https://doi.org/10.1002/eqe.2526

Ghassoun, M. (2020a). An analytical study of the effect of changing vibration amplitudes on the dynamic properties of reinforced concrete bridges (Unpublished doctoral dissertation). Al-Baath University, Syria.

Ghassoun, M., & Alsehnawi, R. (2023). Analytical prediction of damping coefficient-vibration amplitude relationship changes of reinforced concrete bridge piers. Damascus University Journal, 1.

Ghassoun, M., Danhash, G., & Almahmoud, M. (2023). An analytical study of the dynamic responses of high-water tanks in Syria under the effect of the February 2023 earthquake. Journal of the University of Duhok, 26(2). https://doi.org/10.26682/csjuod.2023.26.2.7

Hall, J. F. (2006). Problems encountered from the use (or misuse) of Rayleigh damping. Earthquake Engineering & Structural Dynamics, 35(5), 525-545. https://doi.org/10.1002/eqe.541

Kowalsky, M. J. (1994). Damping in reinforced concrete structures subjected to seismic loading (Master's thesis). University of California, San Diego.

Mahmud, E., & Abdulahad, E. G. (2022). Shaking table tests determining frequency and stiffness before and after strengthening of a confined masonry wall without an opening. In Protection of Historical Constructions. Springer. https://doi.org/10.1007/978-3-030-90788-4_13

Mahmud, E., Bonev, Z., & Abdulahad, E. G. (2019). Nonlinear seismic analysis of masonry infilled RC frame structures. Građevinski materijali i konstrukcije, 62(1), 17-25. https://doi.org/10.5937/GRMK1901017M

Petrini, L., Maggi, C., Priestley, M. J. N., & Calvi, G. M. (2008). Experimental verification of viscous damping modeling for inelastic time history analyses. Journal of Earthquake Engineering, 12(1), 125-145. https://doi.org/10.1080/13632460801925822

Priestley, M. J. N., Calvi, G. M., & Kowalsky, M. J. (2007). Displacement-based seismic design of structures. IUSS Press.

Zareian, F., & Medina, R. A. (2010). A practical method for proper modeling of structural damping in inelastic plane structural systems. Computers & Structures, 88(1-2), 45-53. https://doi.org/10.1016/j.compstruc.2009.08.001

About the authors

MARYAM ALIBRAHEEM

Position at the organization

PhD student at structural civil engineering / Homs University / Homs / Syria

Main research area

Dynamic seismic analysis , Reinforced concrete structures

Address

Homs/Syria
E-mail: m.ibraheem@homs-univ.edu.sy

SOLEMAN ALAMOUDI

Position at the organization

Professor at structural civil engineering / Homs university / Homs / Syria

Main research area

Reinforced concrete analysis and design

Address

Homs/Syria
E-mail: salamodi@homs-univ.edu.sy

This article is an Open Access article distributed under the terms and conditions of the Creative Commons Attribution 4.0 (CC BY 4.0) License (http://creativecommons.org/licenses/by/4.0/).